Available online at www.sciencedirect.com
SCIENCE DIRECT®
International Journal of Heat and Mass Transfer 48 (2005) 2801–2805
International Journal of HEAT and MASS TRANSFER
www.elsevier.com/locate/ijhmt

Technical Note

Heat transfer in an evaporating thin liquid film moving slowly along the walls of an inclined microchannel

Suman Chakraborty [1], S.K. Som *

Department of Mechanical Engineering, Indian Institute of Technology, Kharagpur 721 302, India

Received 9 September 2004; received in revised form 1 January 2005
Available online 31 March 2005

Abstract

A theoretical study has been undertaken to determine the rate of heat transfer in a thin evaporating liquid film flowing along the walls of a microchannel under the combined action of surface tension and gravity. Analytical solutions of conservation equations, in both liquid and vapour phases, have been obtained, in considerations with coupled heat and mass transfer boundary conditions at the interface. It has been recognized that while the local Nusselt number is influenced solely by the liquid film thickness, the average Nusselt number depends both on liquid film thickness and a dimensionless number $\rho g \sin\theta\, \delta_0^2/\sigma$, as obtained from the scale of characteristic velocity for both gravity and surface tension.

1. Introduction

Importance of heat transfer studies of an evaporating thin liquid film originates from the advancement in cooling of microscale electronic devices, and design of microheat pipes. The rate of heat flux in a thin evaporating liquid film in a microdevice depends mainly on the film thickness determined by the imposed condition of flow and the evaporation characteristics at the interface. Several works [1–13] pertaining to numerical and experimental investigations on evaporating thin film are available in the literature. Park and Lee in their recent work [13] has made a brief review of all the pertinent earlier works, which is not repeated here for the purpose of brevity. Most of the earlier models could not properly link the evaporative velocity with mass diffusion in gas phase. The work of Park and Lee [13] considered the effect of disjoining pressure through a dispersion constant, but did not mention about the state of gas phase controlling the interfacial evaporation process. It appears from their work that the gas phase was taken to be a saturated vapor in thermodynamic equilibrium with the liquid film. Under the situation, the phase change phenomenon takes place through the mechanism of boiling to maintain saturated temperature at the interface with a wall superheat, the physics of which is entirely different from that of an evaporation transport.

The present work deals with a thin liquid film maintained throughout at a temperature below the saturation temperature corresponding to its existing pressure, and evaporates from its free surface in a medium of air and water vapor. The rate of evaporation under the situation has been linked with the vapor phase mass diffusion at the interface. The mathematical model is based on the conservation equations for heat, mass and momentum transport in both liquid and vapor phases,

* Corresponding author. Tel./fax: +91 3222 282978.
E-mail addresses: suman@mech.iitkgp.ernet.in (S. Chakraborty), sksom@mech.iitkgp.ernet.in (S.K. Som).
[1] Tel.: +91 3222 282990.

0017-9310/$ - see front matter © 2005 Elsevier Ltd. All rights reserved.
doi:10.1016/j.ijheatmasstransfer.2005.01.030

linked through the interfacial equilibrium conditions. Analytical solutions of such a situation are rarely found in literature, and the present paper has made an attempt towards that direction. The average and local Nusselt number along with the dry out length (i.e., the length of liquid film region from inlet to the location where it vanishes) have been predicted in terms of the pertinent controlling parameters.

2. Mathematical modeling

For the purpose of mathematical modeling, we consider the evaporation phase change phenomenon of a thin liquid film in vicinity of the wall of a microcapillary channel, as depicted in Fig. 1. For geometric similarity, only the lower half is considered for mathematical analysis. Above the liquid film, quiescent air flows at a temperature of T_α, and a moisture concentration of C_α, which has been set to zero for the present study. The channel wall is kept at a constant temperature T_w, which is greater than T_α. The gravity is assumed to act at an angle θ with respect to the negative y-direction. For the sake of analytical treatment, following simplifying assumptions are made:

(1) The transport phenomena are approximately two-dimensional.
(2) Axial (x-direction) diffusion terms in various conservation equations are insignificant in comparison to the transverse (y-direction) diffusion terms, since the characteristic length scale along x-direction is significantly larger in comparison to that along y-direction.
(3) The film thickness (δ) is significantly smaller in comparison to the channel half-width (h).

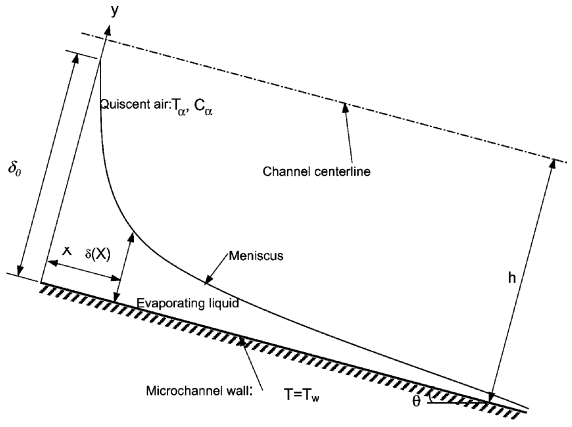

Fig. 1. A schematic diagram of the physical situation.

(4) The axial pressure gradient is a function of x-coordinate only.
(5) Axial gradients of temperature and concentration are relatively inconsequential in comparison to the respective transverse gradients.
(6) Spatial variation of thermophysical properties within the same phase can be neglected, although they are assumed to be different for different phases.
(7) Temperature variation along the y-direction within the liquid phase is assumed to be linear, in consideration of insignificant influence of convection due to small flow velocity in the liquid film.

With the above assumptions, the governing transport equations for the different phases can be written as follows:

(i) Momentum conservation in the liquid phase

$$\mu_l \frac{\partial^2 u}{\partial y^2} = \frac{\partial p}{\partial x} - \rho_l g \sin\theta = -F(x), \quad \text{say} \tag{1}$$

where u is the velocity, p is the pressure, μ is the viscosity, and $F(x)$ is a function of x. In Eq. (1), the subscript 'l' stands for the liquid phase. The above equation is subjected to following boundary conditions:

(a) At $y = 0$, $\quad u = 0$ (2a)

(b) At $y = \delta$, $\quad \dfrac{\partial u}{\partial y} = 0$ (2b)

Eq. (1), subjected to the above boundary conditions, yields

$$u = \frac{l}{2\mu} F(x)[2\delta y - y^2] \tag{3}$$

(ii) Energy conservation in the vapor phase

$$V_s \frac{\partial T}{\partial y} = \alpha_v \frac{\partial^2 T}{\partial y^2} \tag{4}$$

where V_s is the Stefan flow velocity due to evaporation at the interface, and α is the thermal diffusivity. The subscript 'v' indicates a property of the vapor phase. Under the following conditions:

(a) At $y = \delta$, $\quad T = T_s$ (5a)

(b) At $y = h$, $\quad T = T_\alpha$ (5b)

Eq. (4) gives a solution:

$$\frac{T - T_s}{T_s - T_\alpha} = \frac{\exp\left(\frac{V_s y}{\alpha_v}\right) - \exp\left(\frac{V_s \delta}{\alpha_v}\right)}{\exp\left(\frac{V_s \delta}{\alpha_v}\right) - \exp\left(\frac{V_s h}{\alpha_v}\right)} \tag{5}$$

(iii) Species conservation in the vapor phase

$$V_s \frac{\partial C}{\partial y} = D_v \frac{\partial^2 C}{\partial y^2} \tag{6}$$

where C is the concentration of water in the vapor phase, and D_v is the mass diffusivity of vapor in air. Eq. (6) can also be solved analogous to solution of Eq. (4) to yield:

$$\frac{C - C_s}{C_s - C_\alpha} = \frac{\exp\left(\frac{V_s y}{D_v}\right) - \exp\left(\frac{V_s \delta}{D_v}\right)}{\exp\left(\frac{V_s \delta}{D_v}\right) - \exp\left(\frac{V_s h}{D_v}\right)} \tag{7}$$

The above-mentioned equations must be applied in consistency with the appropriate interfacial matching conditions, which are as follows:

(i) The rate of mass transfer at any section x (i.e., $\dot{m}_x$) is related to the rate of evaporation per unit length (i.e., $\dot{m}_e$) as

$$\frac{d\dot{m}_x}{dx} = -\dot{m}_e \tag{8}$$

Using Eq. (3), the above can be simplified to obtain:

$$\delta^3 F'(x) + 3F(x)\frac{d\delta}{dx} = -3\mu\dot{m}_e \tag{9}$$

where

$$\dot{m}_e = \rho_v V_s \tag{9a}$$

(ii) The consideration of interface being impermeable to non-evaporating species gives:

$$\frac{-D_v \frac{\partial C}{\partial y}\Big|_{y=\delta}}{1 - C_s} = V_s \tag{10}$$

Using Eqs. (7) and (10) may be simplified to obtain:

$$V_s = \frac{D_v}{h - \delta} \ln\left(\frac{1 - C_\alpha}{1 - C_s}\right) \tag{11}$$

(iii) The interfacial heat balance (Stefan boundary condition) can be written as

$$-k_v \frac{\partial T_v}{\partial y}\Big|_{y=\delta} + k_l \frac{\partial T_l}{\partial y}\Big|_{y=\delta} = -\rho_v h_{fg} V_s \tag{12}$$

where k is the thermal conductivity, ρ is the density, and h_{fg} is the latent heat of evaporation at the prevailing local conditions. The temperature profile depicted by Eq. (5) can now be substituted in Eq. (12) to obtain a local variation of the interfacial temperature (T_s) as

$$T_s = \frac{-\rho_v h_{fg} V_s + k_l \frac{T_w}{\delta} - T_\alpha f}{\frac{k_l}{\delta} - f} \tag{13}$$

where the function 'f' is given by

$$f = k_v \frac{V_s}{\alpha_v} \frac{\exp\left(\frac{V_s \delta}{\alpha_v}\right)}{\exp\left(\frac{V_s \delta}{\alpha_v}\right) - \exp\left(\frac{V_s h}{\alpha_v}\right)} \tag{13a}$$

The coupled system of Eqs. (9), (11) and (13) can lead to a well-posed problem, subject to the condition that the function $F(x)$ appearing in Eq. (9) is appropriately defined. For this purpose, dynamic conditions prevailing at the interface need to be invoked, described as follows.

(iv) The pressure difference across the interface can be expressed as

$$p - p_\alpha = -\frac{\sigma}{R(x)} + \frac{a}{\sigma^3} \tag{14}$$

where p_α is the pressure in the vapor phase adjacent to the interface, σ is the surface tension coefficient, $R(x)$ is the local interfacial radius of curvature, and a is the dispersion constant [4]. Now, from Eq. (1), we can describe the function $F(x)$, with the help of Eq. (14) as

$$F(x) = -\frac{\sigma}{R^2}\frac{dR}{dx} + \frac{3a}{\delta^4}\frac{d\delta}{dx} + \rho_l g \sin\theta \tag{15}$$

where $R(x)$ is described as

$$R(x) = \frac{\left[1 + \left(\frac{d\delta}{dx}\right)^2\right]^{1.5}}{\frac{d^2\delta}{dx^2}} \tag{15a}$$

In our subsequent analysis, we approximate $R(x)$ by assuming that magnitude of $\left(\frac{d\delta}{dx}\right)^2$ is much smaller in comparison to unity.

It needs to be noted at this point that the interfacial variables T_s, C_s, as well as the term h_{fg}, as appearing in Eqs. (11) and (13) are by no means independent local constants, but are interrelated to each other by pertinent thermodynamic constraints. In the present study, the above thermodynamic constraints are assumed to obey the following relationships [14]:

$$C_s = \frac{l}{1 + \frac{M_{air}}{M_l}\left(\frac{P_{total}}{p_v} - 1\right)} \tag{16a}$$

where M stands for the molecular weight, and the ratio p_{total}/p_v can be obtained from the following relationship:

$$\frac{p_v}{p_{total}} = \exp\left[\frac{\Delta H_{sa}}{R}\left\{\frac{T_s - T_{sa}}{T_s T_{sa}}\right\} - \frac{0.38}{T_c}\ln\frac{T_s}{T_{sa}} - \frac{0.118}{T_c^2}(T_s - T_{sa})\right]. \tag{16b}$$

In Eq. (16b), the subscript 'sa' refers to standard atmospheric conditions, and the subscript 'c' refers to the 'critical state', with all temperatures expressed in K. Further, the variation of h_{fg} can be expressed as [14]:

$$h_{fg} = \Delta H_{sa}\left[\frac{T_c - T_s}{T_c - T_{sa}}\right]^{0.38} \tag{16c}$$

Incorporating the above variations into Eqs. (11) and (13), and substituting those in Eq. (9), a fourth order highly non-linear ordinary differential equation can be obtained, which is solved numerically using the fourth order Runge–Kutta method, by converting the same into a system of four coupled first order equations. The boundary conditions are as follows: at $x = 0$, $\delta = \delta_0$, and as $x \to \infty$ $\delta \to 0$, $d\delta/dx \to 0$, $d^2\delta/dx^2 \to 0$. Finally, we determine the local and average Nusselt number as follows:

$$Nu_x = \frac{h_x x}{k_l} \tag{17}$$

With $h_x = k_l/\delta$, for a linear temperature profile within the liquid, it becomes

$$Nu_x = \frac{x}{\delta} \tag{17a}$$

Analogously, the average Nusselt number is given by

$$\overline{Nu}_{x_d} = \frac{1}{x_d}\int_0^{x_d} Nu_x\,dx = \frac{1}{x_d}\int_0^{x_d} \frac{x}{\delta}\,dx \tag{17b}$$

where x_d is the dry out length (i.e., the length of liquid film region from inlet to the location where it vanishes).

3. Results and discussions

The Fig. 2 shows the variation of local Nusselt number along the length of the channel for different values of δ_0/h. The increase in Nu_x with x is attributed to the decrease in liquid film thickness due to evaporation. It is interesting to note that after a certain distance x, Nu_x blends asymptotically to a very high value. This corresponds to an approximate location of almost dry out region where the liquid film thickness becomes exceedingly small. Since conduction is the dominant mode of heat transfer in the liquid film, the local heat transfer coefficient, for a prescribed temperature difference, is inversely proportional to the film thickness. It is further observed that the distribution of Nu_x for all values of δ_0/h less than or equal to 0.01 fall on a single curve. The variable x (the axial location) is scaled by δ_0 (the initial film thickness) in Fig. 2. Therefore, it is observed from Fig. 2 that the variation of local Nusselt number Nu_x with δ_0, for a given channel height, takes place in a sense that with a change in δ_0, the same value of Nu_x is attained at a value of x that is directly proportional to δ_0.

The rate of heat transfer under the present situation is influenced mainly by the liquid film thickness, which, in turn, is governed by flow velocity and evaporation at the surface. The flow velocity depends on both capillary and gravity forces. A relative magnitude of these two effects can be assessed by a non-dimensional number $\rho g \sin\theta\delta_0^2/\sigma$ obtained from the scale of characteristic velocity for both gravity and surface tension. The Fig. 3 shows that there is a slight decrease in average Nusselt number with the dimensionless parameter $\rho g \sin\theta\delta_0^2/\sigma$. An increase in the parameter $\rho g \sin\theta\delta_0^2/\sigma$ implies either an increase in δ_0 or a decrease in σ, both of which result in an increased film thickness at any given axial location. While the local heat flux depends only on the local film thickness, the total heat transfer from the surface depends on the wetted length (or, dry out length) also, determined by the rate of decay of film thickness along the wall. It is observed from Figs. 4 and 5 that the location of dry out region is almost proportional to the initial film thickness δ_0, but is practically uninfluenced by the surface tension coefficient σ.

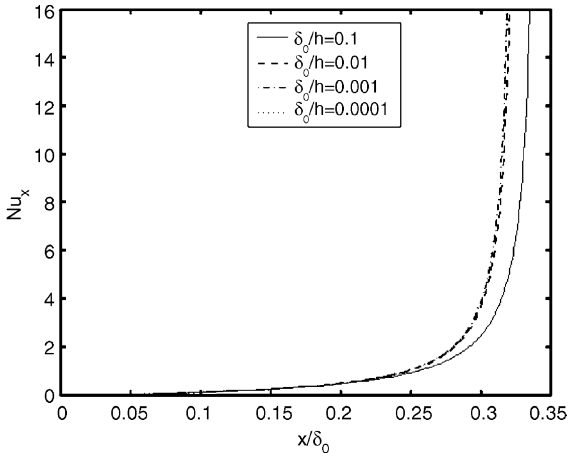

Fig. 2. Axial variation of local Nusselt number.

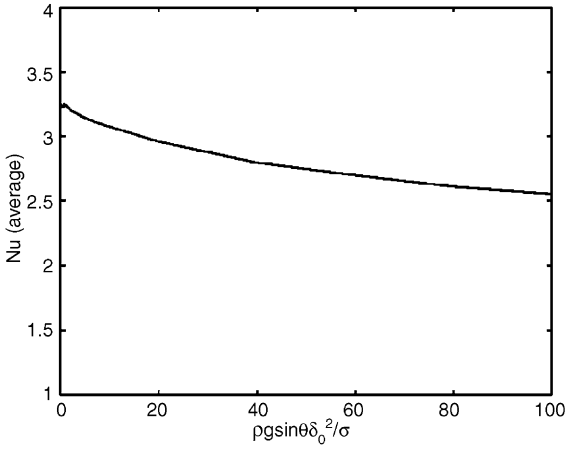

Fig. 3. Variation of average Nusselt number with the dimensionless ratio $\rho g \sin\theta\delta_0^2/\sigma$.

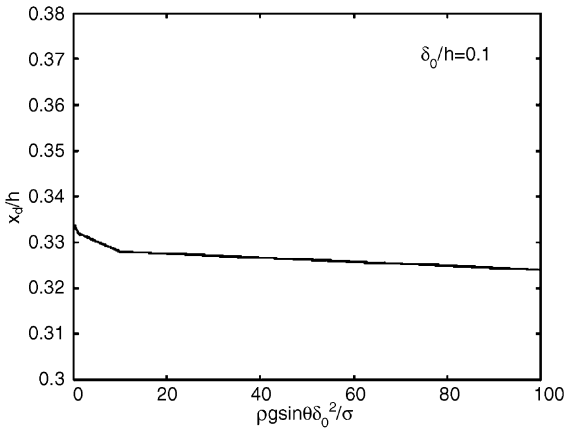

Fig. 4. Location of dry out point as a function of the dimensionless ratio $\rho g \sin\theta \delta_0^2/\sigma$.

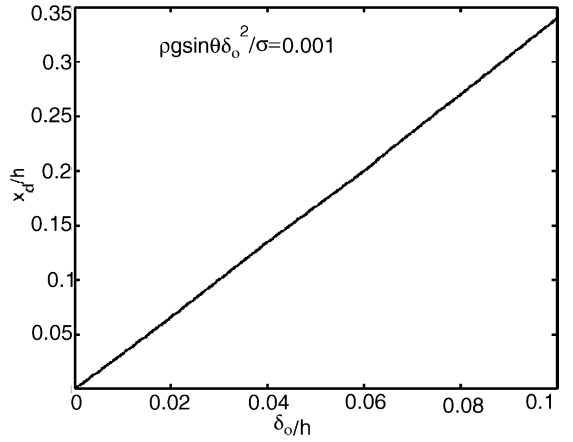

Fig. 5. Location of dry out point as a function of the initial film thickness.

4. Conclusions

Analytical solutions of conservation equations have been made to determine the rate of heat transfer in a thin evaporating liquid film flowing along the walls of a microchannel under the combined action of surface tension and gravity.

While the local Nusselt number is influenced solely by the local thickness of liquid film, the average Nusselt number depends both on liquid film thickness and the dry out length. The local Nusselt number increases gradually along the channel wall but blends asymptotically to a very high value near the dry out region.

The dimensionless number $\rho g \sin\theta \delta_0^2/\sigma$, as obtained from the scale of characteristic velocity for both gravity and surface tension, is found to have a mild inverse relationship with the average Nusselt number. The location of almost dry out region in a channel of a given height is proportional to the initial liquid film thickness.

References

[1] B.V. Derjaguin, S.V. Nerpin, N.V. Churaev, Effect of film transfer upon evaporating liquids from capillaries, RILEM Bull. 29 (1) (1965) 93–98.

[2] F. Blangetti, M.K. Naushahi, Influence of mass transfer on the momentum transfer in condensation and evaporation phenomena, Int. J. Heat Mass Transfer 23 (1980) 1694–1695.

[3] X. Xu, V.P. Carey, Film evaporation from a microgrooved surface—an approximate heat transfer model and its comparison with experimental data, AIAA J. Thermo-Phys. Heat Transfer 4 (4) (1990) 512–520.

[4] S. DasGupta, J.A. Schonberg, P.C. Wayner Jr., Investigation of an evaporating extended meniscus based on the augmented Young–Laplace equation, ASME J. Heat Transfer 115 (1993) 201–210.

[5] J.P. Longtin, B. Badran, F.M. Gerner, A one-dimensional model of a microheat pipe during steady-state operation, ASME J. Heat Transfer 116 (1994) 709–715.

[6] J.H. Lay, V.K. Dhir, Shape of a vapor stem during nucleate boiling of saturated liquids, ASME J. Heat Transfer 117 (1995) 394–401.

[7] J.M. Ha, G.P. Peterson, The interline heat transfer of evaporating thin film along a microgrooved surface, ASME J. Heat Transfer 118 (1996) 747–755.

[8] D. Khrustalev, A. Faghri, Thick-film phenomenon in high heat-flux evaporation from cylindrical pores, ASME J. Heat Transfer 119 (1997) 272–278.

[9] V. Sartre, M. Zaghdoudi, M. Lallemand, Effect of interfacial phenomena on evaporative heat transfer in microheat pipes, Int. J. Therm. Sci. 39 (2000) 498–504.

[10] Y.P. Peles, S. Haber, A steady state, one dimensional model for boiling two phase flow in triangular microchannel, Int. J. Multiphase Flow 26 (2000) 1095–1115.

[11] K. Park, K.J. Noh, K.S. Lee, Transport phenomena in the thin film region of a micro-channel, Int. J. Heat Mass Transfer 46 (2003) 2381–2388.

[12] W. Qu, T. Ma, J. Miao, J. Wang, Effects of radius and heat transfer on the profile of evaporating thin liquid film and meniscus in capillary tubes, Int. J. Heat Mass Transfer 45 (2002) 1879–1887.

[13] K. Park, K.S. Lee, Flow and heat transfer characteristics of the evaporating extended meniscus in a micro-capillary channel, Int. J. Heat Mass Transfer 46 (2003) 4587–4594.

[14] S.P. Sengupta, Theoretical studies on some aspects of droplet and spray evaporation, Ph.D. thesis, Indian Institute of Technology, Kharagpur, 1988.